Clinical Biomechanics 99 (2022) 105745

Contents lists available at ScienceDirect

Clinical Biomechanics

journal homepage: www.elsevier.com/locate/clinbiomech

The relationship between subchondral bone cysts and cartilage health in the Tibiotalar joint: A finite element analysis

Harriet G. Talbott [a], Richard A. Wilkins [b,c], Anthony C. Redmond [b,d], Claire L. Brockett [a,b,d], Marlène Mengoni [a,*]

[a] Institute of Medical and Biological Engineering, School of Mechanical Engineering, University of Leeds, Leeds LS2 9JT, UK
[b] Leeds Institute of Rheumatology & Musculoskeletal Medicine, Chapel Allerton Hospital, Leeds, UK
[c] Leeds haemophilia Comprehensive Care Centre, Leeds Teaching Hospitals NHS trust, Leeds, UK
[d] Versus Arthritis Centre for Sports, Exercise and Osteoarthritis, Nottingham, Oxford, Loughborough, Leeds, UK

ARTICLE INFO

Keywords:
Finite element analysis
Subchondral bone cysts
Hemophilia
Ankle joint
Contact pressure

ABSTRACT

Background: Subchondral bone cysts are a common presentation in ankle haemarthropathy. The relationship with ankle joint health has however not previously been investigated. The aim of this study was to assess the influence of subchondral bone cysts of differing shapes, volumes and depths on joint health.
Methods: Chronologically sequential Magnetic Resonance imaging scans of four hemophilic ankles with subchondral bone cysts present ($N = 18$) were used to build patient specific finite element models under two cystic conditions to assess their influence on cartilage contact pressures. Variables such as location, volume and depth were considered individually, to investigate whether certain cystic conditions may be more detrimental to cartilage health.
Findings: Significant quantifiable contact redistribution was seen in the presence of subchondral bone cysts and this redistribution reflected the shape and size of the cysts, however, with the presence of cysts in both bones in 10 of the 18 cases a direct relationship to volume could not be correlated.
Interpretation: This work demonstrated a redistribution of contact pressures in the presence of subchondral bone cysts. This alteration to loading history could be linked to cartilage degeneration due to the biological response to abnormal loading.

1. Introduction

Haemarthropathy is a consequence of recurrent musculoskeletal bleeds due to hemophilia (Blobel et al., 2015); this joint disease has features in common with both osteo- and rheumatoid arthritis (Blobel et al., 2015; Roosendaal et al., 1999). One such commonality is the presence of Subchondral Bone Cysts (SBCs) – reportedly in the late stages of disease (Lundin et al., 2012).

SBCs are fluid-filled space found within the bone (Plewes, 1940), and can clearly be visualized using magnetic resonance (MR) and computed tomography (CT) imaging due to their contrast with the surrounding bone. Across all disease SBCs present in, the pelvis and long bones of the lower extremities are more common presentation sites in adults, whereas the hands and feet are more often affected in children (Geyskens et al., 2004; Mittal et al., 2011; Purkait et al., 2014). Despite the ankle joint being a common site for SBCs in both adults and children, and the most common site for haemarthropathy (Wilkins et al., 2022), the effect of SBCs on ankle biomechanics has not previously been considered.

The relationship between SBC presence and cartilage health is of interest as abnormal mechanical loading has implications on cartilage maintenance. Variations in intra-articular pressures have been shown to be detrimental to cartilage health, with links reported between high contact pressures and cartilage degeneration (Anderson et al., 2011a), joint immobilization and cartilage damage (Leroux et al., 2001; Säämänen et al., 1987; Setton et al., 1997; Thaxter et al., 1965), and abnormal contact distributions and osteoarthritic changes (Li et al., 2008). Abnormal contact pressures mean the force is not being naturally distributed throughout the joint, which has been linked to reduced cartilage thickness (Van Rossom et al., 2017) and reduced cartilage

* Corresponding author at: Institute of Medical and Biological Engineering, School of Mechanical Engineering, University of Leeds, Leeds LS2 9JT, UK.
E-mail addresses: mnhgt@leeds.ac.uk (H.G. Talbott), R.A.Wilkins@leeds.ac.uk (R.A. Wilkins), A.Redmond@leeds.ac.uk (A.C. Redmond), C.L.Brockett@leeds.ac.uk (C.L. Brockett), M.Mengoni@leeds.ac.uk (M. Mengoni).

https://doi.org/10.1016/j.clinbiomech.2022.105745
Received 21 March 2022; Accepted 22 August 2022
Available online 30 August 2022

stiffness (Carter et al., 2004).

Finite Element (FE) Analysis is a computational tool that is increasingly used in orthopedic applications to assess possible disease progression. Despite the prevalence of SBCs in osteoarthritis (OA) (Audrey et al., 2014; Buckland, 2010; Najefi et al., 2021), rheumatoid arthritis (Rennell et al., 1977), and haemarthropathy (Lundin et al., 2012), very few FE studies have been carried out to assess their influence on joint biomechanics. Both 2D (Dürr et al., 2004) and 3D (Anwar et al., 2020; Frazer et al., 2017; Sarrafpour et al., 2019) analysis have been carried out with varying degrees of simplifications to the SBC properties and shapes. FE has been used to evaluate SBCs in dental applications (Sarrafpour et al., 2019), equine studies (Frazer et al., 2017) and OA (Anwar et al., 2020; Dürr et al., 2004). Only one of these studies has considered what the relationship between SBCs and cartilage might be (Anwar et al., 2020). Size, shape and depth are all variable in SBCs, however have previously been simplified as a circle (Dürr et al., 2004) or sphere (Anwar et al., 2020; Frazer et al., 2017; Sarrafpour et al., 2019) of arbitrary depths from the surface, with volume as the variable of interest. This spherical geometry only accounts for approximately 50% of SBCs, with the remainder presenting irregular shapes (Reilingh et al., 2013). SBC depth varies even within an ankle that has multiple cystic regions, however, this has not been considered in previous FE studies.

This study aimed to use patient specific FE models to assess if there were regions of altered contact pressure that could be associated with SBCs, and whether there was a relationship with any factor relating to SBC geometry or location that would be of greater concern regarding cartilage health.

2. Methods

18 chronologically sequential MRI sequences from four hemophilic ankles with one or more SBC were used to develop 18 image-specific FE models, their equivalent without SBCs, and six additional models with SBCs at different depths. The 42 models were used to investigate: 1) the impact of SBCs on the joint contact pressures (2 × 18 models); 2) the influence of SBC volume (18 models); and 3) the influence of SBC depth (6 models).

2.1. Image information

The MRI data was gathered under local ethical approval MEEC 18–022, following informed consent from the patient or their guardian to use clinical images for research. The four ankles had a range of number of sequences, taken over a range of time periods: 2–7 per ankle, over 28–112 months, for a total of 18 MRI sequences. These sequences were used to measure the location, volume and depth of SBCs using Simpleware ScanIP (version P-2019, Synopsis Inc., Mountain View, California). It was also noted in which bone SBCs were present (14 tibial, 10 talar).

2.2. Patient-specific model development

Segmentation specific meshes for both the tibia and talus, and their respective cartilage components were generated from manual segmentations of each sequence in Simpleware ScanIP. To answer the question as to whether the presence of SBCs influenced the cartilage contact pressures, two conditions were contrasted for each MRI sequence (N = 18); 1) cystic, and 2) intact bone for which the presence of SBCs was ignored in the image segmentation. To generate the cystic models (Fig. 1), an additional segmentation specific mesh was produced for the SBCs present on each MRI scan, and a Boolean operation used to subtract this from the intact bone model.

A total of 36 patient specific FE models were generated (Abaqus 2017, Dassault Systèmes, Vélizy-Villacoublay, FR), and simulated at a position representing neutral standing (Stufkens et al., 2011). 25% patient bodyweight (known for each MRI sequence) was applied through the tibia as this is the proportion of bodyweight anticipated to be transferred through the tibiotalar articulation (Benemerito et al., 2020; Zhang et al., 2020). The distal talus was constrained in all degrees of freedom, and no soft tissue constraints were included.

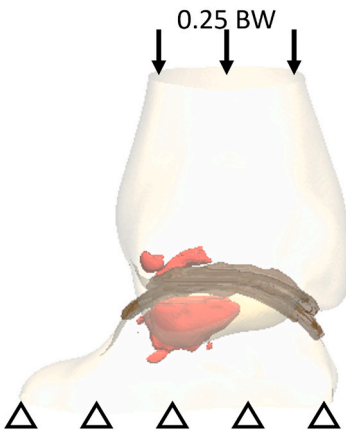

Fig. 1. Loading and boundary conditions to simulate neutral bipedal standing on example ankle model (with segmentation specific SBCs, shown in red, present in both the tibia and the talus). (For interpretation of the references to colour in this figure legend, the reader is referred to the web version of this article.)

In both patient specific model conditions, the bone and cartilage conditions were maintained so that the main sensitivity test was the cystic properties. As the bone outputs were not the primary interest of this study, it was simplified to be homogenous isotropic linear elastic (E = 7.3 GPa, ν = 0.3) (Cheung and Zhang, 2005). The cartilage was modelled as an incompressible Mooney-Rivlin material (C_{10} = 4.5 MPa, C_{01} = 0.66 MPa).

An elastic modulus of 1 MPa was assigned to all cystic tissue, representative of a material much softer than surrounding bone, and the incompressibility the SBC wall would cause was represented with a Poisson's ratio value for the cystic tissue of 0.49 (Frazer et al., 2017; McErlain et al., 2011). These values gave the cystic tissue a bulk modulus of 16.7 MPa, which is relatively low, hence a sensitivity test (supplementary material (Talbott and Mengoni, 2022)) was used to ensure this was not influential on conclusions drawn from this study.

Quadratic tetrahedral elements (C3D10H) were used for all models. A mesh convergence analysis was carried out on one ankle model using both this element type, and linear tetrahedral elements (C3D4), to ensure the element type and mesh densities did not influence the outcomes of the simulation.

2.3. Additional SBC depth study

Given the number of variables for each SBC, additional offset models were generated to assess whether the SBC depth was an important factor on the cartilage mechanics. Six new models from one MRI sequence were generated, each incrementally increasing the SBC offset by +0.5 mm, to a maximum SBC offset of 3 mm. 3 mm was chosen due to this value being towards the upper limit of the range of SBC depths measured

Table 1
SBC properties, including numbers per joint, minimum depths and total volumes, and calculated volume fractions ($\bar{x}$ is the average over the 18 models, S.D. is the standard deviation).

	$\bar{x}$	S.D.	Range
Number of SBCs per ankle	3.17	1.04	2–5
SBC Depth (mm)	0.55	0.9	0–3.9
Total SBC Volume (mm^3)	1944	1441	62–5088
SBC Volume Fraction (%)	6.86	6.06	0.49–22

clinically (Table 1).

2.4. Data analysis

Contact pressure was chosen as the output of interest to investigate the relationship between SBC presence and cartilage health. Statistical testing was carried out using IBM SPSS Statistics (version 26) to 1) calculate the significance of the differences between the two cystic conditions; 2) calculate the correlation between SBC volume and contact pressure; 3) calculate the correlation between SBC volume and contact redistribution; and 4) calculate the correlation between SBC depth and contact pressure. All statistical tests were assigned a 95% confidence interval, and the significance set to 0.05. The tests carried out on contact pressure values were performed for both the peak and mean values.

Wilcoxon's Signed Rank Test was used to calculate the significance of the differences between the two cystic conditions. This non-parametric test was used when Shapiro Wilks testing showed the data was not normally distributed. In the instances that the data was normally distributed, student's *t*-test were used. For the correlations – relating to volume, and depth – Spearman's rank was used, due to the data not clearly showing linearity. In the volume study, the contact pressures from all 18 models were contrasted against their respective total volumes, as well as the volume fractions of the SBCs.

3. Results

SBCs were present on both tibial and talar sides of the tibiotalar joint, with volumes highly variable between ankles and image sequences (Table 1). Full information on the individual SBC volumes, as well as the data derived from FE models, and the supplementary sensitivity study are available as open data from an online repository (Talbott and Mengoni, 2022).

The FE models demonstrated that differences between the two SBC conditions were non-significant for the mean contact pressures (Fig. 2). The difference in the peak tibial cartilage was found to be significant ($p = 0.0004$), but not in the peak talar cartilage ($p = 0.170$).

3.1. SBC volume

The peak and mean contact pressures in the tibial and talar cartilage saw no correlation with the total SBC volume. There were positive but non-significant correlations with the talar SBC volume fractions, and negative but non-significant correlations in the tibial SBC volume fractions (Table 2).

3.2. Stress redistribution

A qualitative redistribution of contact pressures was demonstrated in both cartilage components regardless of where the cystic tissue was found (Fig. 3). The model from which Fig. 3 was produced only had SBCs in the tibia, however, the redistribution can be seen in both tibial and talar cartilages.

The area in contact in both the de facto cystic and intact bone models were normally distributed in both cartilage components ($p = 0.209$ to 0.970). Paired Student's *t*-tests showed the two groups were significantly different in both the tibial cartilage and talar cartilage (both $p < 0.001$). As these differences were significant, the redistribution was quantified by percentage change of area in contact for each cartilage component. The correlation between the percentage change and the total volume were however insignificant ($r_s = -0.152$ and -0.284, tibial and talar changes respectively).

3.3. SBC depth study

Fig. 4 demonstrates how the peak and mean contact pressure changed with the SBC offset in A) tibial and B) talar cartilage. There was a significant negative correlation ($r_s = -0.943$) between the peak tibial contact pressure and the SBC offset, while the correlation for the mean tibial contact pressure was positive but non-significant ($r_s = 0.429$). In the talar cartilage the peak and mean contact pressures both demonstrated very weak negative correlations ($r_s = -0.086$ and -0.290 respectively).

Table 2
Spearman's correlation between total SBC volumes, Talar SBC volume fraction, and Tibial SBC volume fraction in both Tibial and Talar Cartilage contact pressure peak or mean values (CP).

	Tibial Cartilage		Talar Cartilage	
	Peak CP	*Mean CP*	*Peak CP*	*Mean CP*
Total SBC volume	0.084	0.053	0.057	0.024
Talar SBC volume fraction	0.406	0.430	0.394	0.394
Tibial SBC volume fraction	−0.257	−0.138	−0.108	−0.143

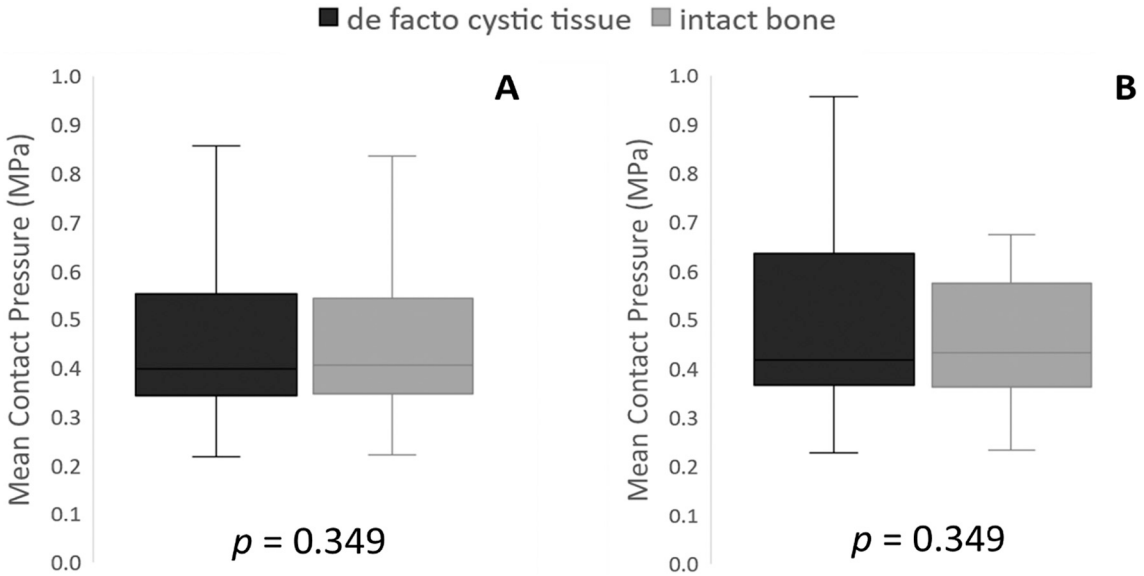

Fig. 2. Difference in mean contact pressure between the two cyst conditions: A) Tibial cartilage, B) Talar cartilage.

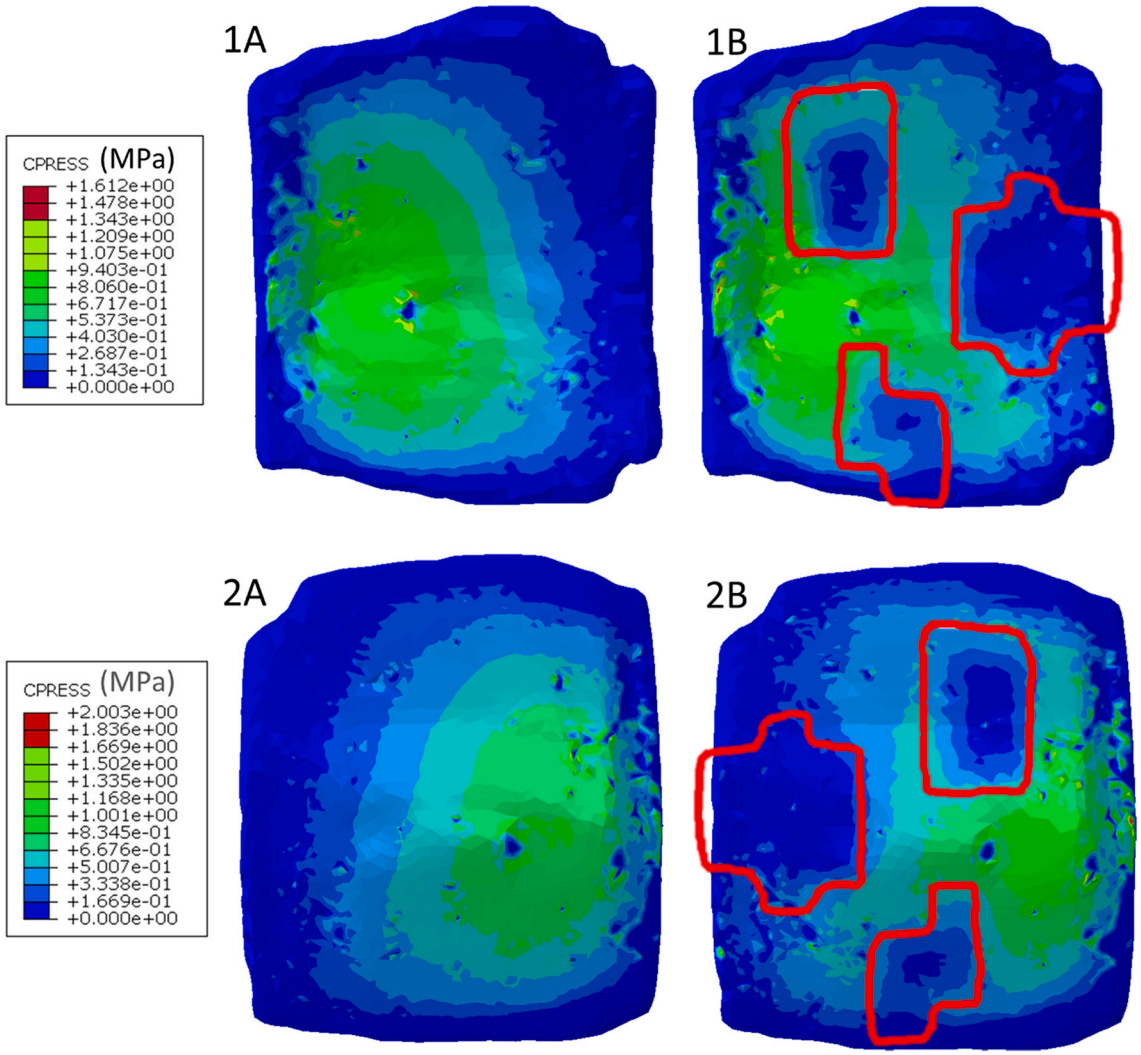

Fig. 3. Contact pressure redistribution in 1) Tibial cartilage, and 2) Talar cartilage. Where (A) represents the intact bone model, and (B) represents the cystic model. Red outline demonstrates location of all SBCs in the model. (For interpretation of the references to colour in this figure legend, the reader is referred to the web version of this article.)

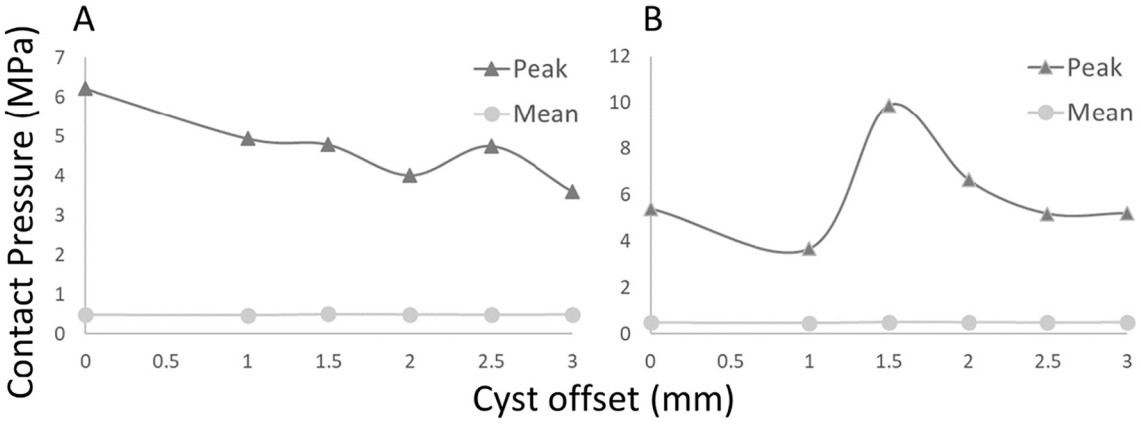

Fig. 4. Peak and mean contact pressure (MPa) in A) tibial and B) talar cartilage with SBC offset.

4. Discussion

Osteoarthritis and haemarthropathy are two distinctly different clinical conditions, however present with similar clinical features, including but not limited to SBCs. Due to these similarities, the models in this study can be used to evaluate cartilage health in both conditions.

The relationship between cartilage pressures, and cartilage health is complicated. Mechanical loading is required for cartilage maintenance,

however, any significant changes in loading history can cause cartilage deterioration (Andriacchi et al., 2004; Brand, 2005). Abnormal mechanical forces and their biologic response play a key role in the onset and progression of post traumatic cartilage loss, with links made previously to both reduced cartilage thickness (Van Rossom et al., 2017) and stiffness (Carter et al., 2004). These disordered properties could in turn trigger further cartilage damage, with potentially irreversible effects.

To the best of the authors' knowledge, this work is the first of its kind to investigate the influence of SBC shape and depth. The results showed that both SBC shape and depth relate to contact pressure redistribution, highlighting the importance of image-specific SBCs in modelling their impact. The lack of significance in the findings related to volume or depth of the SBC does not reflect the redistribution of the contact pressure due to the presence of cysts. The change in contact distribution was seen to occur directly above or below cystic regions, with larger redistribution for larger cysts. Where cysts were present in both bones (10 of the 18 instances), the contact redistribution was not larger than if they had occurred in only in one of the bones, which to some extent explains the lack of correlation between change in contact area and total cyst volume. These findings were based on robust FE models (sensitivity studies available in the data package (Talbott and Mengoni, 2022)), however, are restricted to model-to-model comparisons to negate the lack of experimental validation.

Some simplifications have been made in the methodology to allow these comparisons to be made; ligaments and soft tissues were excluded from the model, and the distal talus was fixed in all degrees of freedom. This would not be representative of the actual ankle joint, but are believed to not significantly influence the contact mechanics and therefore the results of this study. In particular, contact pressure values in this study are similar to those reported through discrete modelling methods at flat foot (Benemerito et al., 2020).

The nature of the clinical MRIs used in this study, with sagittal slice thicknesses of around 3 mm, mean that the SBC volumes generated and measured were an approximation of those occurring within the joint. This estimation is also true of the SBC shape, however, these image based segmentations are less of a simplification than previous spherical SBC geometry.

As it is often the elevation of cartilage pressures that is referred to when considering cartilage degeneration (Anderson et al., 2011a), the non-significant increases in contact pressure when SBCs are present may lead to the conclusion that there is no direct link between SBCs and cartilage degeneration. The redistribution of pressures in both cartilage components could however have their own direct detrimental biological responses with local areas experiencing either increased or decreased contact pressures rather than no change in the local contact pressure.

In mature joints, it has been seen that articular cartilage is thickest and healthiest where the contact pressure and hydrostatic pressure are greatest (Carter et al., 2004). Hydrostatic pressure maintains the chondrocytes in cartilage, which are in turn partially responsible for the maintenance of the extracellular matrix. Supporting the hypothesis that normal pressures are maintaining cartilage health. Given offloaded regions above and below the location of the SBCs may not have the natural maintenance effect, cartilage deterioration could conversely occur, potentially triggering partial or full thickness cartilage loss in those offloaded regions. This study was only carried out to model the ankle mechanics at neutral standing, and to fully understand whether these redistributions occur throughout the whole gait would require inclusion of dynamic gait inputs to the models.

Notable mechanical events that can accelerate joint destruction include genetic related variations (Bálint and Szebenyi, 2000); immobilization (Leroux et al., 2001); and impact, as has been seen in PTOA (Punzi et al., 2016). In studies investigating the pathogenesis of degenerative joint disease, the influence of ageing and mechanical loading on cartilage homeostasis have been considered in conjunction (Mobasheri et al., 2015; Musumeci, 2016). Natural ageing of cartilage is not of relevance to all hemophilic patients (with haemarthropathy onset often happening by the third decade of life (Rodriguez-Merchan, 2010)). Conversely, the exposure of cartilage to blood likely has degenerative pathways overlapping those seen in OA (Pulles et al., 2017). In normal ageing, the deterioration of chondrocyte function undermines cartilage function (Mobasheri et al., 2015). Given chondrocyte apoptosis is also a haemarthritic reaction, it could be concluded that these diseased cartilages may experience the detrimental effect of abnormal contact distribution in the same manner.

The work in the present study did not show changes in mean contact pressure while previous work on the human knee found elevated shear stress directly above cystic regions (Anwar et al., 2020). Both results have implication on cartilage health as the present work demonstrated an abnormal contact distribution where previous work showed abnormal local stress values. Both type of stress outputs can be related to cartilage health. The shear stress and strains have been related to cartilage damage, while the contact pressure is related to pathological changes at the articular surface found in both human OA and experimental models of joint instability (Anderson et al., 2011a; Anderson et al., 2011b; Buckwalter et al., 2013; Li et al., 2008).

Within hemophilia, elevated cartilage pressures have not only been linked to cartilage degeneration, but are hypothesized to be associated with the onset of a joint bleed (Buckwalter and Saltzman, 1999). As these are not significantly increased by SBCs, it would suggest that they do not directly influence bleed onset, therefore we should not expect an increase in ankle bleed rate in patients with SBCs. Patient reported pain should also not be directly linked to SBC presence. However, both could be indirectly linked given the potential for cartilage health decline to be augmented by abnormal pressure distributions due to SBC presence.

5. Conclusions

This work demonstrates that in the presence of ankle haemarthropathy, SBC redistribute joint contact pressures and cartilage loading as SBC properties change over time. These changes confirmed in neutral weight-bearing conditions highlight the potential negative effect of dynamic joint loading on cartilage through the gait cycle during activities of daily living. Where changes to ankle joint structure and function are driven by haemarthropathy, cartilage health decline may accelerate in these offloaded regions, in line with biological response to abnormal cartilage loading.

Role of the funding source

Funding for this research was provided by the Engineering and Physical Sciences Research Council (grant EP/R513258/1, project 2118904). This work was supported by the National Institute for Health Research (NIHR) Biomedical Research Centre in Leeds. The funding body had no involvement with the study submitted in this manuscript.

Declaration of Competing Interest

The authors declare that they have no known competing financial interests or personal relationships that could have appeared to influence the work reported in this paper.

Acknowledgements

The authors would like to thank both the patients for their voluntary participation in this research.

References

Anderson, D.D., Van Hofwegen, C., Marsh, J.L., Brown, T.D., 2011a. Is elevated contact stress predictive of post-traumatic osteoarthritis for imprecisely reduced tibial plafond fractures? J. Orthop. Res. 29, 33–39.

Anderson, D.D., Chubinskaya, S., Guilak, F., Martin, J.A., Oegema, T.R., Olson, S.A., et al., 2011b. Post-traumatic osteoarthritis: improved understanding and opportunities for early intervention. J. Orthop. Res. 29, 802–809.
Andriacchi, T.P., Mündermann, A., Smith, R.L., Alexander, E.J., Dyrby, C.O., Koo, S., 2004. A framework for the in vivo pathomechanics of osteoarthritis at the knee. Ann. Biomed. Eng. 32, 447–457.
Anwar, A., Hu, Z., Zhang, Y., Gao, Y., Tian, C., Wang, X., et al., 2020. Multiple subchondral bone cysts cause deterioration of articular cartilage in medial OA of knee: a 3D simulation study. Front. Bioeng. Biotechnol. 8, 573938.
Audrey, H.X., Abd Razak, H.R.B., Andrew, T.H.C., 2014. The truth behind subchondral cysts in osteoarthritis of the knee. Open Orthop. J. 8, 7–10.
Bálint, G., Szebenyi, B., 2000. Hereditary disorders mimicking and/or causing premature osteoarthritis. Baillieres Best Pract. Res. Clin. Rheumatol. 14, 219–250.
Benemerito, I., Modenese, L., Montefiori, E., et al., 2020. An extended discrete element method for the estimation of contact pressure at the ankle joint during stance phase. J. Eng. Med. 234 (5), 507–516.
Blobel, C.P., Haxaire, C., Kalliolias, G.D., DiCarlo, E., Salmon, J., Srivastava, A., 2015. Blood-induced Arthropathy in hemophilia: mechanisms and heterogeneity. Semin. Thromb. Hemost. 41, 832–837.
Brand, R.A., 2005. Joint contact stress: a reasonable surrogate for biological processes? Iowa Orthop. J. 25, 82–94.
Buckland, J., 2010. It started with a cyst…Or did it? Nature reviews. Rheumatology 6, 310.
Buckwalter, J., Saltzman, C., 1999. Ankle osteoarthritis: distinctive characteristics. Instr. Course Lect. 48, 233–241.
Buckwalter, J.A., Anderson, D.D., Brown, T.D., Tochigi, Y., Martin, J.A., 2013. The roles of mechanical stresses in the pathogenesis of osteoarthritis: implications for treatment of joint injuries. Cartilage 4, 286–294.
Carter, D.R., Beaupré, G.S., Wong, M., Smith, R.L., Andriacchi, T.P., Schurman, D.J., 2004. The mechanobiology of articular cartilage development and degeneration. Clin. Orthop. Relat. Res. S69–S77.
Cheung, J., Zhang, M., 2005. A 3-dimensional finite element model of the human foot and ankle for insole design. Arch. Phys. Med. Rehabil. 86, 353–358.
Dürr, H.D., Martin, H., Pellengahr, C., Schlemmer, M., Maier, M., Jansson, V., 2004. The cause of subchondral bone cysts in osteoarthrosis: a finite element analysis. Acta Orthop. Scand. 75, 554–558.
Frazer, L.L., Santschi, E.M., Fischer, K.J., 2017. The impact of subchondral bone cysts on local bone stresses in the medial femoral condyle of the equine stifle joint. Med. Eng. Phys. 48, 158–167.
Geyskens, W., Vanhoenacker, F.M., Van der Zijden, T., Peerlinck, K., 2004. MR imaging of intraosseous haemophilic pseudotumour: case report and review of the literature. J. Belg. Soc. Radiol. 87, 289–293.
Leroux, M.A., Cheung, H.S., Bau, J.L., Wang, J.Y., Howell, D.S., Setton, L.A., 2001. Altered mechanics and histomorphometry of canine tibial cartilage following joint immobilization. Osteoarthr. Cartil. 9, 633–640.
Li, W., Anderson, D.D., Goldsworthy, J.K., Marsh, J.L., Brown, T.D., 2008. Patient-specific finite element analysis of chronic contact stress exposure after intraarticular fracture of the tibial plafond. J. Orthop. Res. 26, 1039–1045.
Lundin, B., Manco-Johnson, M.L., Ignas, D.M., Moineddin, R., Blanchette, V.S., Dunn, A. L., et al., 2012. An MRI scale for assessment of haemophilic arthropathy from the international prophylaxis study group. Haemophilia 18, 962–970.
McErlain, D.D., Milner, J.S., Ivanov, T.G., Jencikova-Celerin, L., Pollmann, S.I., Holdsworth, D.W., 2011. Subchondral cysts create increased intra-osseous stress in early knee OA: a finite element analysis using simulated lesions. Bone 48, 639–646.
Mittal, S., Arora, S., Khanna, S., Maini, L., Gautam, V.K., 2011. An unusual presentation of haemophilia B: pseudotumor of proximal tibia. Am. J. Orthop. 40, E138–E140.
Mobasheri, A., Matta, C., Zákány, R., Musumeci, G., 2015. Chondrosenescence: definition, hallmarks and potential role in the pathogenesis of osteoarthritis. Maturitas 80, 237–244.
Musumeci, G., 2016. The effect of mechanical loading on articular cartilage. J. Func. Morphol. Kinesiol. 1, 154–161.
Najefi, A.A., Ghani, Y., Goldberg, A.J., 2021. Bone cysts and Osteolysis in ankle replacement. Foot Ankle Int. 42, 55–61.
Plewes, L.W., 1940. Osteo-arthritis of the hip. Br. J. Surg. 27, 682–695.
Pulles, A.E., Mastbergen, S.C., Schutgens, R.E.G., Lafeber, F.P.J.G., van Vulpen, L.F.D., 2017. Pathophysiology of hemophilic arthropathy and potential targets for therapy. Pharmacol. Res. 115, 192–199.
Punzi, L., Galozzi, P., Luisetto, R., Favero, M., Ramonda, R., Oliviero, F., et al., 2016. Post-traumatic arthritis: overview on pathogenic mechanisms and role of inflammation. RMD Open 2, e000279.
Purkait, R., Mukherji, A., Dolai, T.K., Bhadra, R., 2014. Intraosseous Pseudotumour in a child with mild hemophilia B: report of a rare case and brief review of literature. Indian J. Hematol. Blood Transfus. 30, 366–368.
Reilingh, M.L., Blankevoort, L., van Eekeren, I.C., van Dijk, C.N., 2013. Morphological analysis of subchondral talar cysts on microCT. Knee Surg. Sports Traumatol. Arthrosc. 21, 1409–1417.
Rennell, C., Mainzer, F., Multz, C.V., Genant, H.K., 1977. Subchondral pseudocysts in rheumatoid arthritis. Am. J. Roentgenol. 129, 1069–1072.
Rodriguez-Merchan, E.C., 2010. Musculoskeletal complications of hemophilia. HSS J. 6, 37–42.
Roosendaal, Rinsum v, Vianen, Berg vd, Lafeber, Bijlsma, 1999. Haemophilic arthropathy resembles degenerative rather than inflammatory joint disease. Histopathology 34, 144–153.
Säämänen, A.M., Tammi, M., Kiviranta, I., Jurvelin, J., Helminen, H.J., 1987. Maturation of proteoglycan matrix in articular cartilage under increased and decreased joint loading. A study in young rabbits. Connect. Tissue Res. 16, 163–175.
Sarrafpour, B., El-Bacha, C., Li, Q., Zoellner, H., 2019. Roles of functional strain and capsule compression on mandibular cyst expansion and cortication. Arch. Oral Biol. 98, 1–8.
Setton, L.A., Mow, V.C., Müller, F.J., Pita, J.C., Howell, D.S., 1997. Mechanical behavior and biochemical composition of canine knee cartilage following periods of joint disuse and disuse with remobilization. Osteoarthr. Cartil. 5, 1–16.
Stufkens, S.A., Barg, A., Bolliger, L., Stucinskas, J., Knupp, M., Hintermann, B., 2011. Measurement of the medial distal Tibial angle. Foot Ankle Int. 32, 288–293.
Talbott, H.G., Mengoni, M., 2022. [dataset] Subchondral bone cysts in the ankle: patient-specific finite element study data. In: University of Leeds data repository. https://doi.org/10.5518/1207.
Thaxter, T.H., Mann, R.A., Anderson, C.E., 1965. Degeneration of immobilized knee joints in rats: histological and autoradiographic study. JBJS 47.
Van Rossom, S., Smith, C.R., Zevenbergen, L., Thelen, D.G., Vanwanseele, B., Van Assche, D., et al., 2017. Knee cartilage thickness, T1ρ and T2 relaxation time are related to articular cartilage loading in healthy adults. PLoS One 12, e0170002.
Wilkins, R.A., Stephensen, D., Siddle, H., Scott, M.J., Xiang, H., Horn, E., et al., 2022. Twelve-month prevalence of haemarthrosis and joint disease using the Haemophilia joint health score: evaluation of the UK National Haemophilia Database and Haemtrack patient reported data: an observational study. BMJ Open 12, e052358.
Zhang, Y., Chen, Z., Peng, Y., Zhao, H., Liang, X., Jin, Z., 2020. Predicting ground reaction and tibiotalar contact forces after total ankle arthroplasty during walking. J. Eng. Med. 234 (12), 1432–1444.